

Interfacial effects in $\text{La}_{2/3}\text{Sr}_{1/3}\text{MnO}_3$ thin films with different complex oxide capping layers

S. Valencia,^{1,a)} Z. Konstantinovic,² A. Gaupp,¹ D. Schmitz,¹ Ll. Balcells,² and B. Martínez,²

¹Helmholtz-Zentrum-Berlin für Materialien und Energie, Albert-Einstein Str. 15, D-12489 Berlin, Germany

²Instituto de Ciencia de Materiales de Barcelona-CSIC, Campus UAB, E-08193, Bellaterra, Spain

(Presented 17 November 2010; received 24 September 2010; accepted 8 November 2010; published online 25 March 2011)

Interfacial effects in sputtered $\text{La}_{2/3}\text{Sr}_{1/3}\text{MnO}_3$ thin films with different capping layers (MgO, LaAlO_3 , SrTiO_3 , NdGaO_3 , and Au) have been locally investigated by means of x-ray absorption spectroscopy and x-ray magnetic circular dichroism at the Mn $L_{3,2}$ -edge. Data were acquired by using the total electron yield detection mode thus guaranteeing maximum sensitivity to the interface. The data show that LaAlO_3 capping almost does not modify the bulklike Mn valence at the interface. In case of SrTiO_3 and Au, the presence of divalent Mn is detected, whereas MgO and NdGaO_3 capping lead to an increase of the Mn valence oxidation state. The modification of the nominal Mn valence state leads to depressed surface magnetization. © 2011 American Institute of Physics. [doi:10.1063/1.3545814]

INTRODUCTION

The appearance of new states of matter at artificial hetero-interfaces in complex oxides¹ has attracted much attention recently due to its promising perspectives for the implementation of magnetic and magnetoelectronic devices with new and enhanced functionalities. In particular, heterointerfaces between complex oxides with a perovskite structure have resulted in a variety of electronic properties ranging from the formation of a 2D electron gas at the interface between two insulators to the appearance of ferromagnetism at the interface adjoining two nonmagnetic oxides.¹⁻⁵ Those results make evident that the magnetic and electronic properties of oxide based superlattices can be tuned through interfacial effects, such as strain, charge transfer, and spin exchange interactions, and are of major interest for the development of oxide based devices. Interfacial effects are particularly relevant for tunneling devices, such as magnetic tunneling junctions, in which the tunneling current depends critically on the magnetic and electronic properties of the electrode/barrier interface. In this context, the interface of manganite thin films with other complex oxides is of major interest. Several studies that were conducted to analyze the properties of ultrathin manganite films on top of various substrates indicate a dramatic degradation of the magnetotransport properties below a critical thickness.⁶ This degradation usually has been attributed to the existence of phase segregation and disorder at the nanoscale level motivated mainly by structural strain, oxygen stoichiometry, and variations of the chemical composition;^{7,8} however, the role of each of those parameters is far from being well understood. In this context, the use of surface and element-sensitive x-ray spectroscopy techniques could be very helpful for clarifying the microscopic origin of the depression of the magnetotransport properties.^{8,9}

In this work, we report on preliminary results regarding interfacial effects in $\text{La}_{2/3}\text{Sr}_{1/3}\text{MnO}_3$ (LSMO) manganite thin films prepared by sputtering with different capping layers. Capping materials have been selected based on their wide use and their different physical properties (lattice mismatch, band insulators, spin-majority filtering effect, metal), for example, LaAlO_3 (LAO), SrTiO_3 (STO), NdGaO_3 (NGO), MgO, and gold. All LSMO films were grown on (001)-oriented STO substrates, thus guaranteeing identical strain conditions, by using rf magnetron sputtering from stoichiometric ceramic targets. Prior to deposition, substrates were cleaned in an ultrasonic bath with Milli-Q water and annealed at 1000 °C in air for 2 h to obtain a typical morphology of terraces and steps with unit cell height (~ 0.4 nm).⁹ Further details regarding sample preparation can be found elsewhere.¹⁰ The thickness of the samples (~ 50 nm) was determined from grazing incident x-ray reflectometry. The thickness of the capping layers was set to 1.6 (± 0.2) nm and was determined by controlling the evaporation time after a careful calibration of the growth speed of each of the different materials used. Reciprocal space mapping was performed using a Bruker D8 GADDS system equipped with a 2D Hi-Star x-ray detector to determine the degree of strain of the films. Macroscopic magnetic characterization of the samples was performed by using a commercial SQUID magnetometer (Quantum Design).

LSMO has the highest ferromagnetic transition temperature ($T_C \sim 370$ K) among the manganese perovskites with a strong magnetoresistive response and metallic conductivity below T_C . At low temperature, it is a half metal and presents a rhombohedral (R-3c) crystal structure; however, in this work, we will use the pseudocubic notation in which the cell parameter a is $a_{\text{bulk}} = 0.388$ nm. Reciprocal space maps of the (103) reflections of LSMO films grown on STO indicate that an in-plane lattice constant of the LSMO films perfectly matches that of the underlying substrate ($a_{\text{film}} = a_{\text{subst.}} \sim 0.3905$ nm). θ - 2θ scans of the (004) peak of the LSMO samples allow deduction of a c parameter of about 0.3870(3) nm, slightly

^{a)}Author to whom correspondence should be addressed. Electronic mail: sergio.valencia@helmholtz-berlin.de.

smaller than the value of the bulk LSMO material. Thus LSMO films grown on STO substrate are under biaxial tensile strain (+0.41%) with a slightly reduced out-of-plane cell parameter c . Both θ - 2θ scans and reciprocal space maps (not shown) suggest that LSMO films with different capping layers are very homogeneous and uniformly strained throughout the volume.

In Fig. 1, we show the temperature dependence of the magnetization of the different samples measured with an applied magnetic field of 5 kOe. It is found that the ferromagnetic transition temperature, T_C , is very similar in all the samples ($T_C \sim 350$ K) and slightly below that of the bulk material ($T_C \sim 370$ K). Thus we should conclude that capping does not have a severe effect on the robustness of double exchange ferromagnetism in our samples. Only in the case of the sample capped with MgO, does T_C exhibit some extra reduction that deserves further study. On the other hand, it is worth mentioning that saturation magnetization, M_S , shows a clear reduction with respect to the bulk value ($M_S \sim 590$ emu/cm³), and it seems to be correlated with the capping material. However, we should clarify that this is just because samples are not saturated at the field used for $M(T)$ measurements ($H = 5$ kOe). When high magnetic fields ($H \geq 20$ kOe) are applied, M_S values of about 590 emu/cm³ are found in all the cases except for the sample capped with MgO that exhibits a reduction of M_S of about 5%.

To have access to interfacial effects between the film and the capping layer, we have performed both x-ray absorption spectroscopy (XAS) and X-ray magnetic circular dichroism (XMCD) measurements at the Mn $L_{2/3}$ edge. At these photon energies, the radiation probes the unoccupied Mn $3d$ states via $2p \rightarrow 3d$ dipole transitions. The spectroscopic measurements were performed with the 7 Tesla high-field end station at the UE46-PGM1 beamline at the electron storage ring BESSY II. The angle of incidence was set to normal to the surface of the sample. The sample was magnetically saturated along the propagation direction of the radiation applying a magnetic field of 20 kOe. Absorption spectra were measured at $T = 10$ K for right (I^+) and left (I^-) helicities of circularly polarized incident radiation. Total electron yield was used as a detection technique due to its surface sensitivity. The escape depth of the secondary photoelectrons (2–3 nm), as well as the thickness of the capping layers,

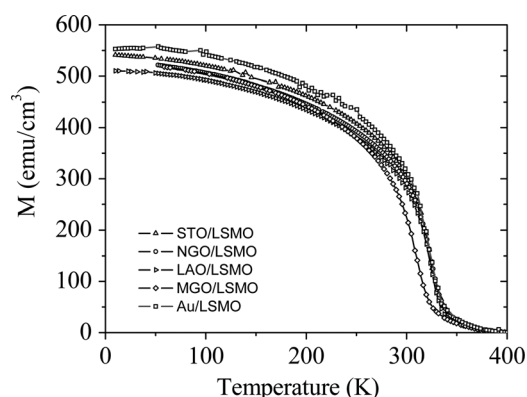


FIG. 1. Magnetization versus temperature, $M(T)$, curves for LSMO samples grown on STO with different capping layers. ($H = 5$ kOe).

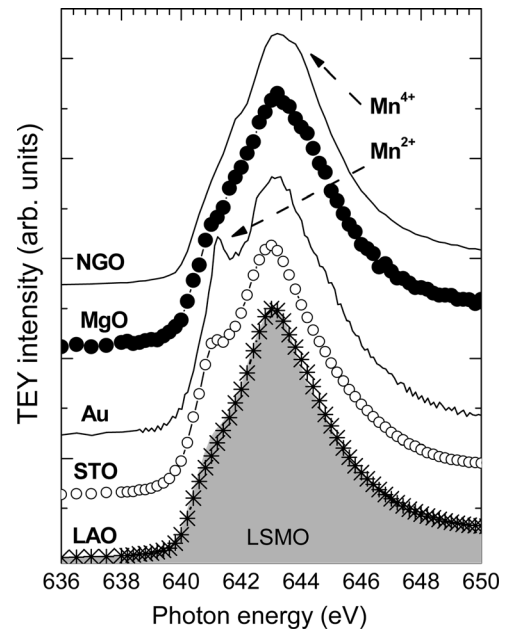


FIG. 2. Mn L_{3} -edge absorption spectra for LSMO thin films with different capping. The reference spectrum is shown by a filled gray curve. Both STO and Au capping lead to a low energy feature associated to Mn^{2+} formation. MgO and NGO cappings promotes the appearance of an excess of Mn^{4+} by the interface, whereas LAO capping does not produce any detectable modification.

guarantees that the measured absorption ($I^+ + I^-$) and thus the XMCD spectrum ($I^+ - I^-$) are mainly determined by the Mn atoms at the interfacial region.

The Mn $L_{3,2}$ spectra of LSMO films with different cappings together with that of uncapped LSMO bulk reference spectrum are depicted in Fig. 2. The LSMO film with LAO capping exhibits an almost bulklike spectrum; nevertheless, some minute differences can be appreciated when compared to the reference sample. A small decrease of intensity is observed at the low energy side of the L_3 peak. According to Abbate *et al.*,¹¹ this can be related to a tiny reduction (increase) of the Mn^{4+} (Mn^{3+}) content at the interface being below 1–2%.

In the case of the STO capping, a slight increase of intensity is observed at the low energy side as compared to the reference sample. Although this could be interpreted as an increase (reduction) of Mn^{3+} (Mn^{4+}), a shift of the spectrum by ca. 0.1 eV to lower energies is also seen. This clearly relates this feature to the presence of divalent Mn.⁹ Following the procedure described in Ref. 9, we can estimate that the LSMO/STO interface contains ca. 6% of Mn^{2+} atoms. The Mn^{2+} promotion is clearer in the case of Au capping. In that case, Mn^{2+} amounts to 14% of the total interfacial Mn atoms.

The other two capping layers studied show notable changes at the high energy side of the L_3 feature with respect to the reference spectrum. Shifts toward higher energy values are also observed for the L_2 peak. This indicates an increase in the oxidation state of the Mn ions, that is, an increase in the Mn^{4+} content at the interface of ca. 18%. A mechanism to explain this increase in the Mn^{4+} content could be, for instance, the formation of $MgMnO_3$.¹²

The XMCD spectral shape of all samples look alike excluding the presence of any ferromagnetic phase besides

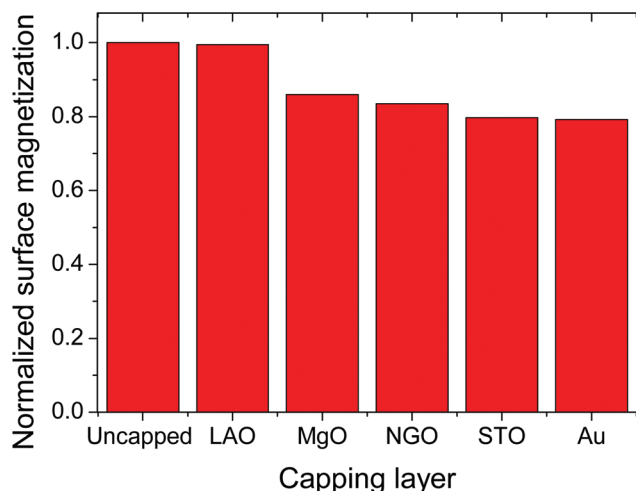


FIG. 3. (Color online) Surface magnetization for LSMO thin films with different capping. Values have been obtained by using the sum rules and normalizing to the uncapped LSMO layer (labeled as uncapped). A reduction of the surface magnetization is detected in those cases where capping also induces modification of the Mn oxidation state at the interface, that is, Au, STO, MgO, and NGO.

that expected according to the nominal composition. Making use of the so-called sum rules,¹³ the contribution of the spin (m_{spin}) and orbital (m_{orb}) moments to the total magnetic moment can be determined. However, in the case of Mn, the sum rules yield values with an error larger than 50% for the spin moment.¹⁴ This prevents, in our case, an exact determination of the interface magnetization; however, a comparative study between the different samples can be safely done. In Fig. 3, we depict the magnetic moment ($m_{\text{spin}} + m_{\text{orb}}$) per atom for the different interfaces normalized to the value obtained for the uncapped (bulklike) sample. Our results indicate that all capping except LAO lead to depressed magnetic moments at the interface in agreement with the departure of the interface Mn oxidation state from the nominal one. This indicates the formation of a secondary nonmagnetic phase at the interface. In the case of Au and STO capping, the decrease of surface magnetization would be in agreement with XAS data showing the existence of Mn^{2+} at the interface. This also agrees with our previously published data where we showed that depressed magnetic properties were concomitant with Mn^{2+} formation.⁹ In the case of MgO and NGO, we observe that the increase in Mn^{4+} content also leads to a depression of surface magnetization.

In conclusion, we have analyzed the effect of different capping layers on the magnetic properties of LSMO films on top of STO substrates while presenting the same strain conditions. As expected, macroscopic measurements do not show any relevant influence of the capping on the magnetic properties since the volume of the sample implicated in the

interface is very small compared to the whole volume of the sample. Nevertheless, an abnormal difference of about 5% in the value of M_S is observed in the case of MgO capping layer; this deserves further studies. However, XAS data demonstrate that the samples are locally modified at the interface in the case of Au and STO showing Mn^{2+} formation and, in the cases of MgO and NGO capping, inducing a Mn^{4+} excess. In contrast LAO capping does not seem to disturb the interface. XMCD results are in agreement with XAS showing depressed interfacial magnetization in those cases where there is a clear departure from the bulklike Mn oxidation state. For LAO capping, robust ferromagnetic ordering survives at the interface.

ACKNOWLEDGMENTS

We acknowledge financial support from the Spanish MEC (MAT2009-08024 and MAT2008-04931/NAN), CONSOLIDER (CSD2007-00041) and FEDER program. The research leading to these results has received funding from the European Community's Seventh Framework Program (FP7/2007-2013) under Grant No. 226716. Z.K. thanks the Spanish MEC for the financial support through the RyC program.

¹A. Ohtomo and H. Hwang, *Nature (London)* **427**, 423 (2004).

²M. Huijben, G. Rijnders, D. H. A. Blank, S. Bals, S. Van Aert, J. Verbeeck, G. Van Tendeloo, A. Brinkman, and H. Hilgenkamp, *Nat. Mater.* **5**, 556 (2006).

³H. Yamada, Y. Ogawa, Y. Ishii, H. Sato, M. Kawasaki, H. Akoh, and Y. Tokura, *Science* **305**, 646 (2004).

⁴S. Thiel, G. Hammerl, A. Schmehl, C. W. Schneider, and J. Mannhart, *Science* **313**, 1942 (2006).

⁵A. Brinkman, M. Huijben, M. van Zalk, J. Huijben, U. Zeitler, J. C. Maan, W. G. van der Wiel, G. Rijnders, D. H. A. Blank, and H. Hilgenkamp, *Nat. Mater.* **6**, 493 (2007).

⁶M. Bibes, S. Valencia, Ll. Balcells, B. Martínez, J. Fontcuberta, M. Wojcik, S. Nadolski, and E. Jedryka, *Phys. Rev. B* **66**, 134416 (2002); M. Angeloni, G. Balestrino, N. G. Boggio, P. G. Medaglia, P. Orgiani, and A. Tebano, *J. Appl. Phys.* **96**, 6387 (2004).

⁷E. Dagotto, *Science* **309**, 257 (2005)

⁸Ll. Abad, V. Laukhin, S. Valencia, A. Gaupp, W. Gudat, Ll. Balcells, and B. Martínez, *Adv. Funct. Mater.* **17**, 3918 (2007).

⁹S. Valencia, A. Gaupp, W. Gudat, Ll. Abad, Ll. Balcells, A. Cavallaro, B. Martínez, and F. J. Palomares, *Phys. Rev. B* **73**, 104402 (2006); S. Valencia, A. Gaupp, W. Gudat, Ll. Abad, Ll. Balcells, and B. Martínez, *Phys. Rev. B* **75**, 184431 (2007).

¹⁰Z. Konstantinovic, J. Santiso, D. Colson, A. Forget, Ll. Balcells, and B. Martínez, *J. Appl. Phys.* **105**, 5 (2009)

¹¹M. Abbate, F. M. F. de Groot, J. C. Fuggle, A. Fujimori, O. Strebel, F. Lopez, M. Domke, G. Kaindl, G. A. Sawatzky, M. Takano, Y. Takeda, H. Eisaki, and S. Uchida, *Phys. Rev. B* **46**, 4511 (1992).

¹²B. L. Chamberland, A. W. Sleight, and J. F. Weiher, *J. Solid State Chem.* **1**, 512 (1970).

¹³B. T. Thole, P. Carra, F. Sette, and G. van der Laan, *Phys. Rev. Lett.* **68**, 1943 (1992); P. Carra, B. T. Thole, M. Altarelli, and X. D. Wang, *Phys. Rev. Lett.* **70**, 694 (1993).

¹⁴C. Piamonteze, P. Miedema, and F. M. F. de Groot, *Phys. Rev. B* **80**, 184410 (2009) and references therein.